Communications in Computational Chemistry
Commun. Comput. Chem., Vol. 7, No. 3, 243–248
doi: 10.4208/cicc.2025.217.01

Regular Article

Comparison Between All-Atom and Coarse-Grained Dynamics Simulations for Predicting Mechanical Properties of Proteins

Zihan He[1], Liangxu Xie[2,*], Binbin Xie[3] and Lin Shen[1,*]

[1] *Key Laboratory of Theoretical and Computational Photochemistry of Ministry of Education, College of Chemistry, Beijing Normal University, Beijing 100875, China;*

[2] *Institute of Bioinformatics and Medical Engineering, School of Electrical and Information Engineering, Jiangsu University of Technology, Changzhou 213001, Jiangsu, China;*

[3] *Hangzhou Institute of Advanced Studies, Zhejiang Normal University, Hangzhou 311231, Zhejiang, China.*

[*] Corresponding authors: lshen@bnu.edu.cn; xieliangxu@jsut.edu.cn

Received on 5 August 2025; Accepted on 15 August 2025

Abstract: In this work, we perform all-atom and coarse-grained dynamics simulations to predict the mechanical properties of a typical synthetic protein system. Previous experiments showed that proteins with a larger molecular weight exhibit better mechanical performance. Our steered molecular dynamics (SMD) simulations at the all-atom level only capture intermolecular interactions and fail to reproduce this tendency. The results of the dissipative particle dynamics (DPD) simulations at the coarse-grained level are consistent with experiments. The comparison between two levels of resolution highlights the importance of simulation scales in predicting mechanical properties of complex systems. We also reveal some underlying factors correlated with the mechanical properties of synthetic proteins, such as molecular weights, fabrication processes, the ratio of hydrophobic to hydrophilic segments and their order in the amino acid sequences.

Key words: steered molecular dynamics, dissipative particle dynamics, mechanical property, silk protein, multiscale simulation.

One of the central tasks of computational chemistry is predicting physical and chemical properties. Since many chemical processes occur in a broad range of spatial and time scales, the level of resolution for simulations is crucial for computational models [1-5]. On one hand, predictions on optoelectronic properties of materials require explicit modelling of electronic degrees of freedom that are governed by quantum mechanics. On the other hand, thermodynamic properties such as the free energy changes during biological processes can be well predicted based on classical statistical mechanics via molecular dynamics (MD) simulations. How to improve the accuracy and efficiency of simulations with affordable computational resources has been a long-standing challenge. Compared with the all-atom computational model, the coarse-grained model reduces particular degrees of freedom and significantly saves computational cost, usually at the expense of prediction accuracy. In practice, all-atom MD simulation results can be utilized as the reference to validate the thermodynamic properties predicted at the coarse-grained level.

Aside from optoelectronic and thermodynamic properties, theoretical predictions on the mechanical properties of complex molecular systems are also an important task of computational chemistry, especially for the rational design of biomaterials. In recent years, various computational models at different levels of resolution have been developed and successfully applied to study the mechanical properties of proteins, microtubules and other types of polymers [6-10]. However, a comprehensive comparison of all-atom and coarse-grained simulation results has never been discussed in depth, at least to the best of our knowledge. In the present work, we

implemented molecular simulations for synthetic silk proteins to predict their mechanical properties at the all-atom and coarse-grained levels. The difference between these two computational models was illustrated in Figure 1.

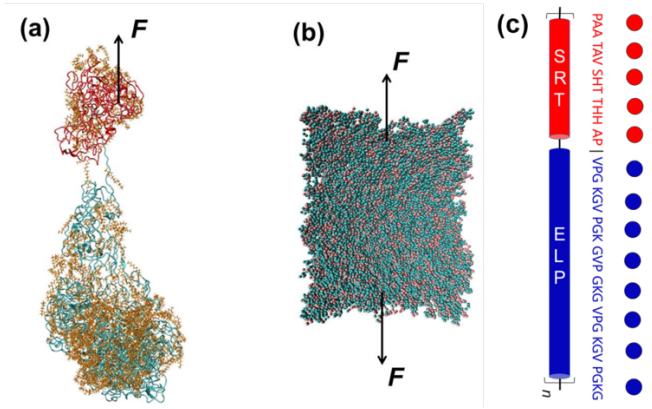

Figure 1. Computational models: SMD at all-atom level (a), DPD at coarse-grained level (b), and an example of mapping between two levels (c).

We employed recombinant chimeric proteins consisting of the squid ring teeth (SRT) and elastin-like polypeptide (ELP) sequences, which have been studied by Liu and coworkers in experiments [11-13], as our test systems. The SRT acts as a hydrophobic segment with the sequence of PAATAVSHTTHHAP, while the ELP is a hydrophilic sequence as $(VPGKG)_5$. These two segments repeat several times to construct silk proteins, such as $(SRT\text{-}ELP)_{12}$, $(SRT\text{-}SRT\text{-}ELP)_9$, $(SRT\text{-}ELP\text{-}ELP)_7$, $(SRT\text{-}ELP)_{24}$ and $(SRT\text{-}ELP)_{36}$. It was observed in experiments that the polymer of SRT-ELP with a larger molecular weight exhibits better mechanical performance, including a higher breaking stress and Young's modulus [11]. The impact of fabrication processes such as the introduction of glutaraldehyde crosslinking or non-covalent counterion surfactants was also well investigated experimentally and theoretically [11,14], revealing details of intermolecular interactions. However, the theoretical prediction of the mechanical properties of such complex systems is still challenging.

We first applied steered molecular dynamics (SMD) simulations to four systems: $(SRT\text{-}ELP)_{12}$, $(SRT\text{-}SRT\text{-}ELP)_9$, $(SRT\text{-}ELP\text{-}ELP)_7$ and $(SRT\text{-}ELP)_{24}$ with sodium dodecyl benzenesulfonates (SDBSs) at the all-atom level. The results were depicted in Figure 2. The standard deviations were small relative to the corresponding average values, justifying the setup of SMD simulations. The breaking stresses predicted for 12mer and 24mer were 315 and 227 kJ/mol/nm, respectively. Notably, the breaking stress decreases with the growing molecular weight, which is opposite to experimental observations [11]. Then we compared the results of $(SRT\text{-}SRT\text{-}ELP)_9$, $(SRT\text{-}ELP\text{-}ELP)_7$ and $(SRT\text{-}ELP)_{12}$ since their molecular weights are similar. The breaking stress was predicted as 344 and 278 kJ/mol/nm for $(SRT\text{-}SRT\text{-}ELP)_9$ and $(SRT\text{-}ELP\text{-}ELP)_7$, respectively, exhibiting an increased order of breaking stresses as $(SRT\text{-}ELP\text{-}ELP)_7 < (SRT\text{-}ELP)_{12} < (SRT\text{-}SRT\text{-}ELP)_9$. It suggests that the SRT segment with β-sheet structures may enhance the tensile strength of proteins via hydrogen bonds and hydrophobic interactions with other chains, while the ELP segment may be more relevant to conformational variability. Taking account of the serious deviation from experiments, however, any conclusion based on the present all-atom MD simulations is questionable in the absence of independent theoretical verifications.

The limitations of all-atom MD simulations, including molecular modelling, equilibrium sampling and umbrella pulling, may be responsible for the unsatisfactory results. First, the three-dimensional protein structures should be predicted from the amino acid sequence at the beginning. Such a homology modelling process is a nontrivial issue for synthetic proteins. Second, different protein force fields probably generate different conformational ensembles [15,16], but the influence on mechanical proteins still lies in the lack of research.

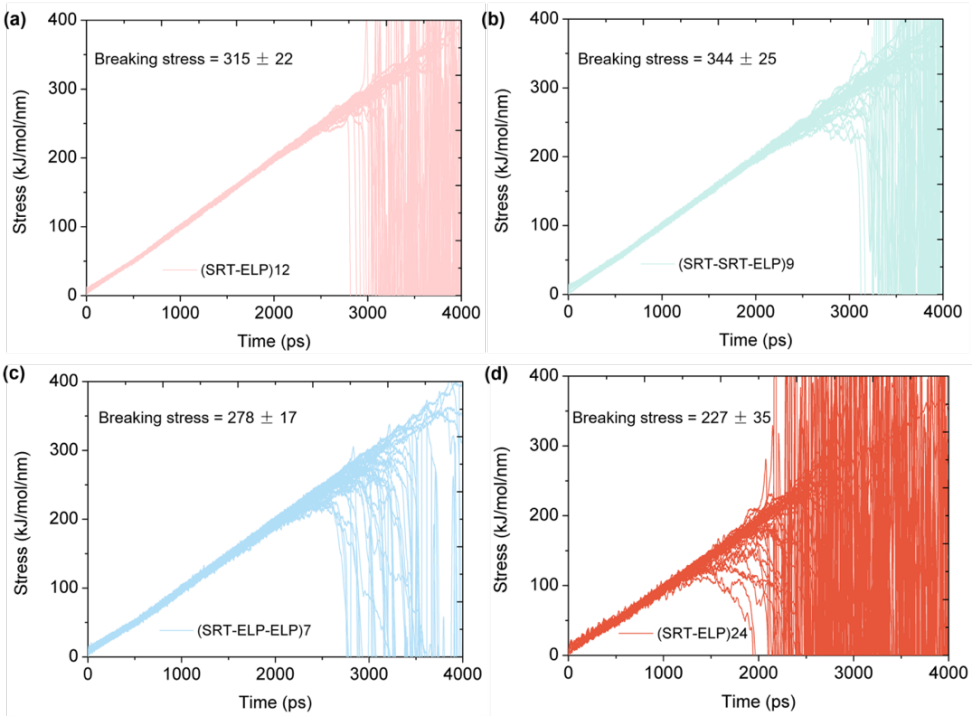

Figure 2. Stress curves as a function of SMD simulation time with breaking stresses of different systems: $(SRT\text{-}ELP)_{12}$ (a), $(SRT\text{-}SRT\text{-}ELP)_9$ (b), $(SRT\text{-}ELP\text{-}ELP)_7$ (c), and $(SRT\text{-}ELP)_{24}$ (d).

Third, the non-covalent interactions between protein chains (possibly via SDBSs as counterion surfactants) dominate the slowest motion. It is difficult for a normal MD to explore the vast conformational space or achieve sufficient sampling. Finally, SMD simulations on only five protein chains cannot represent the mechanical characterization of fibers in experiments. Although the rapid development of the AlphaFold [17,18] and enhanced sampling techniques [19,20] has provided extensive solutions to the first three problems, the last limitation is mainly due to the intrinsic gap between dynamic simulations at the microscopic scale and mechanical properties measured at the macroscopic scale. How to bridge this gap is still an open question.

We turned to dissipative particle dynamics (DPD) simulations that have been used for studying the mechanical properties of silk fibers by Buehler, Wong and their coworkers at a mesoscopic resolution [21]. Five systems were first studied: $(SRT\text{-}ELP)_{12}$, $(SRT\text{-}SRT\text{-}ELP)_9$, $(SRT\text{-}ELP\text{-}ELP)_7$, $(SRT\text{-}ELP)_{24}$ and $(SRT\text{-}ELP)_{36}$. Taking account of different characteristic scales in experiments and simulations, we focused on the relative order of predicted Young's modulus rather than the absolute values. The results were summarized in Figure 3. First, the Young's modulus is increased with molecular weight, which is in good agreement with experimental observations [11]. It suggests that the enlarged protein system can lead to the growth of intermolecular interactions. The atomic details have been observed in our all-atom MD trajectories, involving the electrostatic interactions between the phenylsulfonate of SDBS and the lysine in ELP, and the hydrophobic interactions between the long-chain alkane of SDBS and the proline in SRT. Second, we compared the results with and without the shearing process (as well as the following compressive stage) during DPD simulations. The predictions of the 12mer, 24mer and 36mer show that the degree of increase in Young's modulus is more considerable after a shear flow. In contrast, a saturated Young's modulus becomes evident from the 24mer to the 36mer. It highlights the importance of fabrication that may modulate the network connectivity by shearing. Finally, the ranking order of mechanical properties: $(SRT\text{-}ELP\text{-}ELP)_7 < (SRT\text{-}ELP)_{12} < (SRT\text{-}SRT\text{-}ELP)_9$ was observed again, supporting the aforementioned conclusion of SMD simulations on different roles of SRT and ELP segments in synthetic silk proteins. Although it is still difficult for all-atom SMD simulations to reproduce the trend of mechanical properties with the growing sizes of proteins, the relative ranking order of the predicted breaking stresses of different systems with similar molecular weights appears to be reliable. It is worth noting that Pérez and coworkers compared four atomistic force fields for mechanical properties of double-stranded DNA recently, and reconciled these differences via a single mapping between sequence-dependent conformation and elasticity [22]. We thus inferred that improvement of all-atom force fields is probably not a priority for studying mechanical properties of proteins. Further work is required to validate this finding

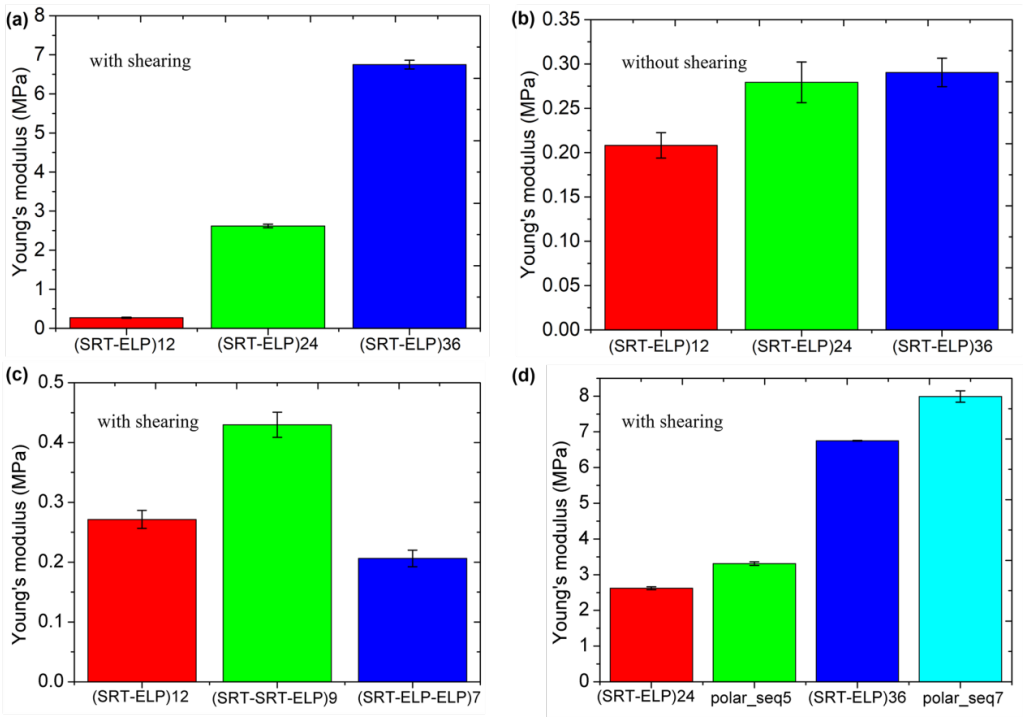

Figure 3. Young's modulus of different systems obtained from DPD simulations: SRT-ELP polymers with shearing (a), SRT-ELP polymers without shearing (b), SRT-ELP polymers with different ratios of hydrophobic to hydrophilic segments (c), and different patterns of amino acid sequences (d). Note that the ranges of the vertical axes in different subfigures are different.

The aforementioned results indicate that hydrophobic segments play a positive role, while hydrophilic segments play a negative role, in enhancing the mechanical properties of proteins. However, it was observed experimentally that charged amino acids in a silk protein (e.g., mussel foot protein) facilitates mechanical properties [23,24]. We built two systems comprising a long chain of B beads and a short chain of A beads: $(B_{20}\text{-}(BBBBAABBBAABBBB)_2\text{-}B_{20})_5$ and $(B_{20}\text{-}(BBBBAABBBAABBBB)_2\text{-}B_{20})_7$, to study this issue. These two sequences share similar molecular weights of $(SRT\text{-}ELP)_{24}$ and $(SRT\text{-}ELP)_{36}$, respectively. We denoted them as polar_seq5 and polar_seq7. The DPD simulation results were shown in Figure 3d. The positive correlation between mechanical properties and molecular weights remains the same. The Young's modulus of polar_seq5 and polar_seq7 were about 20% higher than those of

$(SRT\text{-}ELP)_{24}$ and $(SRT\text{-}ELP)_{36}$, respectively, suggesting a new pattern of amino acid sequence for de novo protein design. Our simulations at the coarse-grained level reveal that not only the ratio of hydrophobic to hydrophilic segments but also their order in the sequence influences the mechanical properties of silk proteins.

Despite the better prediction performance of DPD simulations compared to SMD simulations, the resolution at the coarse-grained level still has inherent weaknesses, leaving much room for improvement. First, amino acid mutation is a powerful tool for designing mechanically biological structural proteins. However, one bead for DPD simulations represents nine water molecules and thus corresponds to three amino acid residues [25]. Such a low level of resolution makes the modelling of amino acid mutation impossible. It requires modifications on the coarse-grained model in which one residue should be mapped to at least one bead, but the reparameterization is always a laborious task under existing techniques. Second, our comparison between SMD and DPD lacks rigor without reconstruction of all-atom details from mesoscopic structures. Considering the huge size of simulation boxes (e.g., the 36mer in the DPD model corresponds to 0.01 billion atoms), a common back-mapping reconstruction is too expensive. Combination with artificial intelligence models such as the AlphaFold provides an opportunity to deal with these systems. The existing experimental data about mechanical properties can be employed as an auxiliary label for fine-tuning, which may further enhance the performance of currently used artificial intelligence models for mechanical proteins.

In summary, we have predicted the mechanical properties of the typical synthetic silk proteins using two simulation methods: SMD at the all-atom level and DPD at the coarse-grained level. Counterintuitively, the all-atom SMD cannot reproduce the experimental observations, while the results using the coarse-grained DPD are in good qualitative agreement with the experiments. It suggests that the scale of molecular dynamics simulation may play a more important role than the level of resolution in the theoretical prediction of mechanical properties, at least for the synthetic protein systems under study.

Methodology

Simulation Details of SMD. Take the $(SRT\text{-}ELP)_{12}$ as an example. The well-established iterative threading assembly refinement (I-TASSER) server [26-28] was employed to predict the three-dimensional structure of the trimer since its crystal structure is unavailable. Based on this prediction, the structure of the 12mer can be obtained manually. In the first stage of simulations, water molecules were added to the simulation box, making sure that the minimum distance between the box boundary and protein atoms was set as the cutoff distance for nonbonded interactions. After energy minimization and pre-equilibrium MD simulations under the NVT and NPT ensembles lasting for 500 ps, respectively, we carried out 50 ns NPT MD simulations at the room temperature and pressure to achieve sufficient sampling of 12mer. In the second stage, five snapshots of the 12mer protein were extracted and compacted to a larger simulation box. Since a pulling force would be applied to the 12mer protein in the next stage and would lead to an expansion of the protein system, we increased the minimum distance between the box boundary and protein by two-thirds in this stage. Then 300 sodium ions, 300 chloride ions, and 500 SDBSs were added to the box. Note that the systems consist of five 12mer chains as well as hundreds of counterion surfactants. Energy minimization, pre-equilibrium NVT and NPT MD simulations, and long-time NPT MD simulations were subsequently carried out with the same procedure as that used in the first stage. In the final stage, we implemented SMD simulations under the NVT ensemble, in which one 12mer chain was pulled out of four others using a harmonic potential with the force constant of 100 kJ/mol/nm^2. The pulling procedure was independently applied to each of the five chains 50 times to obtain stress curves as a function of simulation time as well as breaking stresses. The integration time step was set as 2 fs for all above simulations. The velocity rescaling thermostat [29] and Parrinello-Rahman barostat [30] were used. The cutoff distance for nonbonded interactions was set as 12 Å, and the long-range electrostatic interactions were represented using the particle mesh Ewald (PME) approach [31]. The CHARMM36 force field, CGenFF and TIP3P model were applied to proteins, ions and SDBSs, and waters, respectively [32-34]. All simulations at the all-atom level were performed with the Gromacs software package [35].

Simulation Details of DPD. Unlike many other coarse-grained protein force fields such as MARTINI, here only two types of beads are defined to represent the hydrophobic (denoted as A) and hydrophilic (denoted as B) domains of proteins. In addition, the W bead represents the coarse-grained level of resolution for 9 water molecules. In DPD simulations, the total force acting on bead I is a sum over all other beads J within a cutoff distance R_c, that is

$$F_I = \sum_{J \neq I} \left(F_{IJ}^C + F_{IJ}^D + F_{IJ}^R \right) \quad (1)$$

where F^C, F^D and F^R represent the conservative force, dissipative force and random force, respectively. The dissipative and random forces together form a thermostat at the room temperature. The conservative force depends on the intrinsic properties of simulated systems and consists of three terms in this study: repulsion interaction, hydrogen-bonding interaction, and bead-spring interaction along chains. More details of these forces and their parameterization can be seen from the original literature [21,25].

The related characteristic length scale (R_c) and time scale (τ) in DPD were 9.321 Å and 0.75 ns, respectively. As shown in Figure 1c, each SRT and ELP segment was mapped to 5 A beads and 8 B beads, respectively. The box sizes were $120R_c$, $80R_c$ and $40R_c$, in which a unit volume was filled with an average of three beads. The fraction of water was set as 10% according to experimental conditions. The time step of DPD simulations was set as 0.03τ. The pre-equilibrium simulation was first implemented for 630,000 time steps, followed by 420,000 steps to mimic the fiber-spinning process with the Lee-Edwards boundary condition and a shear rate of $0.01\tau^{-1}$ along the x axis (normal to the y axis). The compressive simulation with a negative strain rate of $-5.0 \times 10^{-6}\ \tau^{-1}$ along the x axis was required to relax the system until the residual stress generated during the shearing process could be ignored. The tensile process was finally performed for 100,000 time steps with a strain rate of $7.5 \times 10^{-6}\ \tau^{-1}$ along the x axis. The Young's modulus (denoted as E_x) can be obtained from the linear region of the stress-strain curve as follows

$$E_x = \frac{\sigma_x - 0.5\left(\sigma_y + \sigma_z\right)}{\varepsilon_x} \quad (2)$$

Here σ_k and ε_k denote the stress and strain along the k axis ($k = x$, y or z), respectively. All simulations at the coarse-grained level were implemented using the LAMMPS software package [36].

Acknowledgments

We are grateful to the financial support from the National Key Research and Development Program of China (No. 2019YFA0709400), Natural Science Foundation of China (No. 22003020), the Key Science and Technology Project of Jinhua City (2023-1-093), and the Zhejiang Provincial Natural Science Foundation of China (No. LZ23B030001).

References

[1] Senn H.M. and Thiel W., QM/MM methods for biomolecular systems. *Angew. Chem. Int. Ed.,* **48** (2009), 1198–1229.

[2] Meier K., Choutko A., Dolenc J., Eichenberger A.P., Riniker S. and van Gunsteren W.F., Multi-resolution simulation of biomolecular systems: a review of methodological issues. *Angew. Chem. Int. Ed.,* **52** (2013), 2820–2834.

[3] Zhou H.-X., Theoretical frameworks for multiscale modeling and simulation. *Curr. Opin. Struct. Biol.,* **25** (2014), 67–76.

[4] van Gunsteren W.F. and Oostenbrink C., Methods for classical-mechanical molecular simulation in chemistry: achievements, limitations, perspectives. *J. Chem. Inf. Model.,* **64** (2024), 6281–6304.

[5] Capone M., Romanelli M., Castaldo D., Parolin G., Bello A., Gil G. and Vanzan M., A vision for the future of multiscale modeling. *ACS Phys. Chem. Au,* **4** (2024), 202–225.

[6] Pasi M., Lavery R. and Ceres N., PaLaCe: a coarse-grain protein model for studying mechanical properties. *J. Chem. Theory Comput.,* **9** (2013), 785–793.

[7] López Barreiro D., Yeo J., Tarakanova A., Martin-Martinez F.J. and Buehler M.J., Multiscale modeling of silk and silk-based biomaterials—a review. *Macromol. Biosci.,* **19** (2018), 1800253.

[8] Zha J.-Y., Zhang Y.-W., Xia K.-L., Gräter F. and Xia F., Coarse-grained simulation of mechanical properties of single microtubules with micrometer length. *Front. Mol. Biosci.,* **7** (2021), 632122.

[9] Donets S., Guskova O. and Sommer J.-U., Searching for aquamelt behavior among silklike biomimetics during fibrillation under flow. *J. Phys. Chem. B,* **125** (2021), 3238–3250.

[10] Kim J., Zhang Y., Burgula S., Zha R.H. and Shi Y., Molecular dynamics simulation of self-assembly and tensile deformation of silk-mimetic polymers. *Biomacromolecules,* **26** (2025), 2852–2867.

[11] Li Y., Li J., Sun J., He H., Li B., Ma C., Liu K. and Zhang H., Bioinspired and mechanically strong fibers based on engineered non-spider chimeric proteins. *Angew. Chem. Int. Ed.,* **59** (2020), 8148.

[12] Zhang X., Li J., Ma C., Zhang H. and Liu K., Biomimetic structural proteins: modular assembly and high mechanical performance. *Acc. Chem. Res.,* **56** (2023), 2664–2675.

[13] Su R., Ma C., Han B., Zhang H.-J. and Liu K., Proteins for hyperelastic materials. *Small,* **21** (2025), 2406388.

[14] Xiao L., Wang Z., Sun Y., Li B., Wu B., Ma C., Petrovskii V.S., Gu X., Chen D., Potemkin I.I., et al., An artificial phase-transitional underwater bioglue with robust and switchable adhesion performance. *Angew. Chem. Int. Ed.,* **133** (2021), 12189–12196.

[15] Guvench O. and MacKerell Jr. A.D., Comparison of protein force fields for molecular dynamics simulations. *Methods Mol. Biol.,* **443** (2008), 63–88.

[16] Wang A., Zhang Z. and Li G., Higher accuracy achieved in the simulations of protein structure refinement, protein folding, and intrinsically disordered proteins using polarizable force fields. *J. Phys. Chem. Lett.,* **9** (2018), 7110–7116.

[17] Jumper J., Evans R., Pritzel A., Green T., Figurnov M., Ronneberger O., Tunyasuvunakool K., Bates R., Žídek A., Potapenko A., et al., Highly accurate protein structure prediction with AlphaFold. *Nature,* **596** (2021), 583–589.

[18] Varadi M., Bertoni D., Magana P., Paramval U., Pidruchna I., Radhakrishnan M., Tsenkov M., Nair S., Mirdita M., Yeo J., et al., AlphaFold protein structure database in 2024: providing structure coverage for over 214 million protein sequences. *Nucleic Acids Res.,* **52** (2024), 368–375.

[19] Yang Y.I., Shao Q., Zhang J., Yang L. and Gao Y.Q., Enhanced sampling in molecular dynamics. *J. Chem. Phys.,* **151** (2019), 070902.

[20] Mehdi S., Smith Z., Herron L., Zou Z. and Tiwary P., Enhanced sampling with machine learning. *Annu. Rev. Phys. Chem.,* **75** (2024), 347–370.

[21] Lin S., Ryu S., Tokareva O., Gronau G., Jacobsen M.M., Huang W., Rizzo D.J., Li D., Staii C., Pugno N.M., et al., Predictive modelling-based design and experiments for synthesis and spinning of bioinspired silk fibres. *Nat. Commun.,* **6** (2015), 6892.

[22] Roldán-Piñero C., Luengo-Márquez J., Assenza S. and Pérez R., Systematic comparison of atomistic force fields for the mechanical properties of double-stranded DNA. *J. Chem. Theory Comput.,* **20** (2024), 2261–2272.

[23] Sun J., Su J., Ma C., Göstl R., Herrmann A., Liu K. and Zhang H., Fabrication and mechanical properties of engineered protein-based adhesives and fibers. *Adv. Mater.,* **32** (2020), 1906360.

[24] Li J., Jiang B., Chang X., Yu H., Han Y. and Zhang F., Bi-terminal fusion of intrinsically-disordered mussel foot protein fragments boosts mechanical strength for protein fibers. *Nat. Commun.,* **14** (2023), 2127.

[25] Rim N.-G., Roberts E.G., Ebrahimi D., Dinjaski N., Jacobsen M.M., Martín-Moldes Z., Buehler M.J., Kaplan D.L. and Wong J.Y., Predicting silk fiber mechanical properties through multiscale simulation and protein design. *ACS Biomater. Sci. Eng.,* **3** (2017), 1542–1556.

[26] Zhang Y., I-TASSER server for protein 3D structure prediction. *BMC Bioinformatics,* **9** (2008), 40.

[27] Roy A., Kucukural A. and Zhang Y., I-TASSER: a unified platform for automated protein structure and function prediction. *Nat. Protoc.,* **5** (2010), 725–738.

[28] Zheng W., Zhang C., Li Y., Pearce R., Bell E.W. and Zhang Y., Folding non-homologous proteins by coupling deep-learning contact maps with I-TASSER assembly simulations. *Cell Rep. Methods,* **1** (2021), 100014.

[29] Bussi G., Donadio D. and Parrinello M., Canonical sampling through velocity rescaling. *J. Chem. Phys.,* **126** (2007), 014101.

[30] Parrinello M. and Rahman A., Polymorphic transitions in single crystals: a new molecular dynamics method. *J. Appl. Phys.,* **52** (1981), 7182–7190.

[31] Darden T., York D. and Pedersen L., Particle mesh Ewald: an N·log(N) method for Ewald sums in large systems. *J. Chem. Phys.,* **98** (1993), 10089.

[32] Huang J. and MacKerell A.D., CHARMM36 all-atom additive protein force field: validation based on comparison to NMR data. *J. Comput. Chem.,* **34** (2013), 2135–2145.

[33] Vanommeslaeghe K., Hatcher E., Acharya C., Kundu S., Zhong S., Shim J., Darian E., Guvench O., Lopes P., Vorobyov I. and MacKerell Jr. A.D., CHARMM general force field: a force field for drug-like molecules compatible with the CHARMM all-atom additive biological force fields. *J. Comput. Chem.,* **31** (2010), 671–690.

[34] Jorgensen W.L., Chandrasekhar J., Madura J.D., Impey R.W. and Klein M.L., Comparison of simple potential functions for simulating liquid water. *J. Chem. Phys.,* **79** (1983), 926–935.

[35] Abraham M.J., Murtola T., Schulz R., Páll S., Smith J.C., Hess B. and Lindahl E., GROMACS: high performance molecular simulations through multi-level parallelism from laptops to supercomputers. *SoftwareX,* **1–2** (2015), 19–25.

[36] Thompson A.P., Aktulga H.M., Berger R., Bolintineanu D.S., Brown W.M., Crozier P.S., in't Veld P.J., Kohlmeyer A., Moore S.G. and Nguyen T.D., LAMMPS—a flexible simulation tool for particle-based materials modeling at the atomic, meso, and continuum scales. *Comput. Phys. Commun.,* **271** (2022), 108171